

The measurement programme at the neutron time-of-flight facility n_TOF at CERN

F. Gunsing^{1,2,a}, O. Aberle², J. Andrzejewski³, L. Audouin⁴, V. Bécaries⁵, M. Bacak^{1,2,6}, J. Balibrea-Correa⁵, M. Barbagallo⁷, S. Barros⁸, F. Bečvář⁹, C. Beinrucker¹⁰, F. Belloni¹, E. Berthoumieux¹, J. Billowes¹¹, D. Bosnar¹², A. Brown²⁹, M. Brugger², M. Caamaño¹³, F. Calviño¹⁴, M. Calviani², D. Cano-Ott⁵, R. Cardella², A. Casanovas¹⁴, D.M. Castelluccio^{15,16}, F. Cerutti², Y.H. Chen⁴, E. Chiaveri², N. Colonna⁷, M.A. Cortés-Giraldo¹⁷, G. Cortés¹⁴, L. Cosentino¹⁸, L.A. Damone^{7,19}, K. Deo²⁰, M. Diakaki^{1,21}, C. Domingo-Pardo²², R. Dressler²³, E. Dupont¹, I. Durán¹³, B. Fernández-Domínguez¹³, A. Ferrari², P. Ferreira⁸, P. Finocchiaro¹⁸, R.J.W. Frost¹¹, V. Furman²⁴, S. Ganesan²⁰, A.R. García⁵, A. Gawlik³, I. Gheorghe²⁵, S. Gilardoni², T. Glodariu²⁵, I.F. Gonçalves⁸, E. González⁵, A. Goverdovski²⁶, E. Griesmayer⁶, C. Guerrero¹⁷, K. Göbel¹⁰, H. Harada²⁷, T. Heftrich¹⁰, S. Heinitz²³, A. Hernández-Prieto^{2,14}, J. Heyse²⁸, D.G. Jenkins²⁹, E. Jericha⁶, F. Käppeler³⁰, Y. Kadi², A. Kalamara²¹, T. Katabuchi³¹, P. Kavargin⁶, V. Ketlerov²⁶, V. Khryachkov²⁶, A. Kimura²⁷, N. Kivel²³, M. Kokkoris²¹, M. Krtička⁹, D. Kurtulgil¹⁰, E. Leal-Cidoncha¹³, C. Lederer^{32,10}, H. Leeb⁶, J. Leredegui¹⁷, M. Licata^{16,33}, S. Lo Meo^{15,16}, S.J. Lonsdale³², R. Losito², D. Macina², J. Marganiec^{3,39}, T. Martínez⁵, A. Masi², C. Massimi^{16,33}, P. Mastinu³⁴, M. Mastroianni⁷, F. Matteucci^{35,36}, E.A. Mauger²³, A. Mazzone^{7,37}, E. Mendoza⁵, A. Mengoni¹⁵, P.M. Milazzo³⁵, F. Mingrone^{2,16}, M. Mirea²⁵, S. Montesano², A. Musumarra^{18,38}, R. Nolte³⁹, A. Negret²⁵, A. Oprea²⁵, F.R. Palomo-Pinto¹⁷, C. Paradela¹³, N. Patronis⁴⁰, A. Pavlik⁴¹, J. Perkowski³, I. Porras^{2,42}, J. Praena^{17,42}, J.M. Quesada¹⁷, D. Radeck³⁹, K. Rajeev²⁰, T. Rauscher^{43,44}, R. Reifarth¹⁰, A. Riego-Perez¹⁴, M. Robles¹³, P. Rout²⁰, C. Rubbia², J.A. Ryan¹¹, M. Sabaté-Gilarte^{2,17}, A. Saxena²⁰, P. Schillebeeckx²⁸, S. Schmidt¹⁰, D. Schumann²³, P. Sedyshev²⁴, A.G. Smith¹¹, N.V. Sosnin¹¹, A. Stamatopoulos²¹, S.V. Suryanarayana²⁰, G. Tagliente⁷, J.L. Tain²², A. Tarifeño-Saldivia^{14,22}, D. Tarrío¹³, L. Tassan-Got⁴, A. Tsinganis^{2,21}, S. Valenta⁹, G. Vannini^{16,33}, V. Variale⁷, P. Vaz⁸, A. Ventura¹⁶, V. Vlachoudis², R. Vlastou²¹, A. Wallner⁴⁵, S. Warren¹¹, M. Weigand¹⁰, C. Weiss^{2,6}, C. Wolf¹⁰, P.J. Woods³², T. Wright¹¹, P. Žugec^{2,12}, and the n_TOF Collaboration (www.cern.ch/ntof)

¹ CEA Saclay, Irfu, Gif-sur-Yvette, France

² European Organization for Nuclear Research (CERN), Switzerland

³ University of Lodz, Poland

⁴ Institut de Physique Nucléaire, CNRS-IN2P3, Univ. Paris-Sud, Université Paris-Saclay, 91406 Orsay Cedex, France

⁵ Centro de Investigaciones Energéticas Medioambientales y Tecnológicas (CIEMAT), Spain

⁶ Technische Universität Wien, Austria

⁷ Istituto Nazionale di Fisica Nucleare, Sezione di Bari, Italy

⁸ Instituto Superior Técnico, Lisbon, Portugal

⁹ Charles University, Prague, Czech Republic

¹⁰ Johann-Wolfgang-Goethe Universität, Frankfurt, Germany

¹¹ University of Manchester, UK

¹² University of Zagreb, Croatia

¹³ University of Santiago de Compostela, Spain

¹⁴ Universitat Politècnica de Catalunya, Spain

¹⁵ Agenzia nazionale per le nuove tecnologie (ENEA), Bologna, Italy

¹⁶ Istituto Nazionale di Fisica Nucleare, Sezione di Bologna, Italy

¹⁷ Universidad de Sevilla, Spain

¹⁸ INFN Laboratori Nazionali del Sud, Catania, Italy

¹⁹ Dipartimento di Fisica, Università degli Studi di Bari, Italy

²⁰ Bhabha Atomic Research Centre (BARC), India

²¹ National Technical University of Athens, Greece

²² Instituto de Física Corpuscular, Universidad de Valencia, Spain

²³ Paul Scherrer Institut (PSI), Villigen, Switzerland

²⁴ Joint Institute for Nuclear Research (JINR), Dubna, Russia

²⁵ Horia Hulubei National Institute of Physics and Nuclear Engineering, Romania

²⁶ Institute of Physics and Power Engineering (IPPE), Obninsk, Russia

²⁷ Japan Atomic Energy Agency (JAEA), Tokai-mura, Japan

^ae-mail: gunsing@cea.fr

- ²⁸ European Commission JRC, Institute for Reference Materials and Measurements, Retieseweg 111, 2440 Geel, Belgium
²⁹ University of York, UK
³⁰ Karlsruhe Institute of Technology, Germany
³¹ Tokyo Institute of Technology, Japan
³² School of Physics and Astronomy, University of Edinburgh, UK
³³ Dipartimento di Fisica e Astronomia, Università di Bologna, Italy
³⁴ Istituto Nazionale di Fisica Nucleare, Sezione di Legnaro, Italy
³⁵ Istituto Nazionale di Fisica Nucleare, Sezione di Trieste, Italy
³⁶ Dipartimento di Astronomia, Università di Trieste, Italy
³⁷ Consiglio Nazionale delle Ricerche, Bari, Italy
³⁸ Dipartimento di Fisica e Astronomia, Università di Catania, Italy
³⁹ Physikalisch Technische Bundesanstalt, Braunschweig, Germany
⁴⁰ University of Ioannina, Greece
⁴¹ Universität Wien, Austria
⁴² University of Granada, Spain
⁴³ Centre for Astrophysics Research, University of Hertfordshire, UK
⁴⁴ Department of Physics and Astronomy, University of Basel, Switzerland
⁴⁵ Australian National University, Canberra, Australia

Abstract. Neutron-induced reaction cross sections are important for a wide variety of research fields ranging from the study of nuclear level densities, nucleosynthesis to applications of nuclear technology like design, and criticality and safety assessment of existing and future nuclear reactors, radiation dosimetry, medical applications, nuclear waste transmutation, accelerator-driven systems and fuel cycle investigations. Simulations and calculations of nuclear technology applications largely rely on evaluated nuclear data libraries. The evaluations in these libraries are based both on experimental data and theoretical models. CERN's neutron time-of-flight facility n_TOF has produced a considerable amount of experimental data since it has become fully operational with the start of its scientific measurement programme in 2001. While for a long period a single measurement station (EAR1) located at 185 m from the neutron production target was available, the construction of a second beam line at 20 m (EAR2) in 2014 has substantially increased the measurement capabilities of the facility. An outline of the experimental nuclear data activities at n_TOF will be presented.

1. Introduction

Nuclear data in general, and neutron-induced reactions in particular, are important for a number of research fields. Evaluated nuclear reaction data play an essential role in calculations and simulations for design and operational studies of nuclear technology systems. For this purpose they have to contain all reactions and all energy regions, even where experimental data are missing, insufficient or inconsistent. Applications of nuclear data are usually based on evaluated nuclear data libraries like JEFF, ENDF, JENDL, CENDL, BROND and several others. While these libraries have started historically with a focus on nuclear fission reactors, nowadays they are general purpose libraries and intended to be universal.

Experimental data form an important source of information for evaluated nuclear data. The EXFOR library [1,2] is the international storage and retrieval system for experimental results. It contains data that are often not available numerically in publications and laboratory reports. The measured quantities including detailed experimental conditions have nowadays become the standard quality for EXFOR submission.

Contributions to nuclear data come from a variety of experimental facilities, including the pulsed white spallation neutron source n_TOF at CERN, which has been recently upgraded with its second beam line [3,4]. Each facility has its own unique and often complementary characteristics. A more complete overview of the nuclear data measurements and their references performed at n_TOF since the start of its scientific measurement programme in 2001 is given in Ref. [5].

2. The neutron time-of-flight facility n_TOF at CERN

The neutron time-of-flight facility n_TOF was constructed following an idea proposed by Rubbia et al. [6] and has become fully operational after a commissioning programme [7]. The facility is based on the 6 ns wide, 20 GeV pulsed proton beam from CERN's Proton Synchrotron (PS) with typically 7×10^{12} protons per pulse, impinging on a lead spallation target, yielding about 300 neutrons per incident proton. A layer of water around the spallation target moderates the initially fast neutrons down to a white spectrum of neutrons covering the full range of energies between meV and GeV.

The neutron bunches are spaced by multiples of 1.2 s, a characteristic of the operation cycle of the PS. This allows measurements to be made over long times of flight, reaching to low neutron energies, without any overlap into the next neutron cycle. In this way it is possible to measure neutron energies as low as about 10 meV, with the neutron spectrum free of slow neutrons from previous cycles. The large energy range that can be measured at once is one of the key characteristics of the facility.

Another important feature of n_TOF is the very high number of neutrons per proton burst, also called instantaneous neutron flux. In case of cross section measurements on radioactive samples in the neutron beam, this results in a favourable ratio between the number of signals due to neutron-induced reactions and those due to radioactive decay events contributing to the background.

Two different target-moderator assemblies have been used up to now in the operation of n_TOF. A first spallation target was used from 2001 up to 2004 during

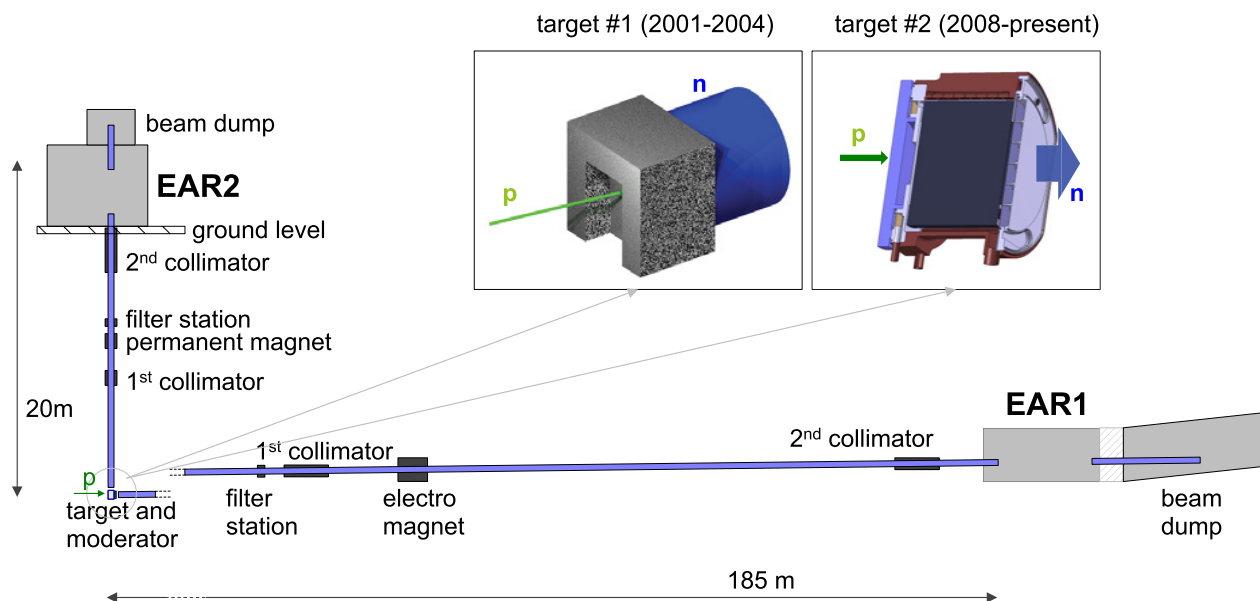


Figure 1. Impression of the n_TOF facility with its two neutron beam lines (drawn in blue) ending in the experimental areas EAR1 and EAR2. The neutron source, on the left lower part of the drawing, is a lead spallation target on which the proton beam (in green) impinges. In the direction of EAR1 a separate neutron moderator is located. The two different targets that have been used up to now are shown in the top insets (surrounding cooling water omitted, see text).

phase-I. The water coolant of the target also served as a neutron moderator. The spallation target was a block of lead of dimensions $80 \times 80 \times 60 \text{ cm}^3$. During phase-II, after the installation in 2008 of an upgraded cylindrical lead spallation target 40 cm in length and 60 cm in diameter, the target was enclosed with a separate cooling circuit resulting in a 1 cm water layer in the neutron beam direction, followed by an exchangeable moderator with a thickness of 4 cm. Demineralized water has been used as a moderator, as well as water with a saturated ^{10}B -solution in order to reduce the number of 2.223 MeV gamma rays from hydrogen capture, which otherwise forms an important contribution to the background due to in-beam gamma rays. The ^{10}B -loaded moderator, strongly suppressing thermal neutrons, affects the energy distribution of the neutron flux only noticeably below 1 eV.

Since the construction of EAR2 in 2014 two neutron beam lines are in operation. In Fig. 1 a sketch of the two beam lines is shown, together with insets showing the two spallation targets used up to now. The corresponding neutron fluxes, per unit of lethargy, are shown in Fig. 2. The higher flux density of EAR2 compared to EAR1, a factor of about 25 with the flux expressed in neutrons/eV/pulse, opens the possibility for measurements on targets of low mass or for reactions with low cross section within a reasonable time. The shorter flight distance of about a factor 10 also results in a 10 times shorter time interval for a same energy region. Therefore, the combination of the higher flux and the shorter time interval results in an increase of the signal to noise ratio of a factor 250 (flux expressed in neutrons/ns/pulse) for radioactive samples, at cost of lower energy resolution. The strong suppression of the thermal neutron peak in EAR1 due to the ^{10}B -loaded moderator is clearly visible in Fig. 2. The horizontal neutron beam line, collimated and guided through an evacuated tube over a distance of approximately 185 m, has been in use since the start of the facility. It leads to an experimental area (EAR1)

where samples and detectors can be mounted and neutron induced reactions are measured. A second neutron beam line and experimental area (EAR2), has been constructed and has been operational since 2014. This flight path is vertical and about 20 m long, viewing the top part of the spallation target. In this case the cooling water circuit acts as a moderator.

3. Nuclear data measurements at n_TOF

A substantial number of nuclear data measurements has been performed at n_TOF. For a full list with references, see Ref. [5]. One of the major issues to overcome is the availability of radioactive samples in a suitable form for neutron time-of-flight measurements [8,9].

During phase-I from 2001 to 2004, data have been taken for a number of nuclides in capture and fission experiments. These include neutron capture measurements on the nuclei $^{24,25,26}\text{Mg}$, ^{56}Fe , $^{90,91,92,93,94,96}\text{Zr}$, ^{139}La , ^{151}Sm , $^{186,187,188}\text{Os}$, ^{197}Au , $^{204,206,207,208}\text{Pb}$, ^{209}Bi , ^{233}U , ^{234}U , ^{237}Np , ^{240}Pu , and ^{243}Am with C_6D_6 detectors and with a 4π total absorption calorimeter (TAC) consisting of 40 BaF_2 crystals. The spatial neutron beam profile, needed for normalization of the neutron flux, has been measured with a MicroMegas-based detector (MGAS) [10] and was confirmed by simulations, allowing the energy-dependent beam-interception factor to be calculated.

Fission ionization chambers (FIC) were used to measure the fission cross sections of the actinides ^{232}Th , ^{234}U , ^{236}U , and ^{237}Np relative to ^{235}U and ^{238}U . An additional chamber was used to measure neutron-induced fission cross sections of the very radioactive actinides ^{233}U , ^{241}Am , ^{243}Am , and ^{245}Cm , also relative to ^{235}U , ^{238}U .

In addition fission detectors based on Parallel Plate Avalanche Counters (PPACs) were developed, simultaneously detecting both fission fragments, which allows to discard alpha and high-energy reactions and therefore being capable of performing fission

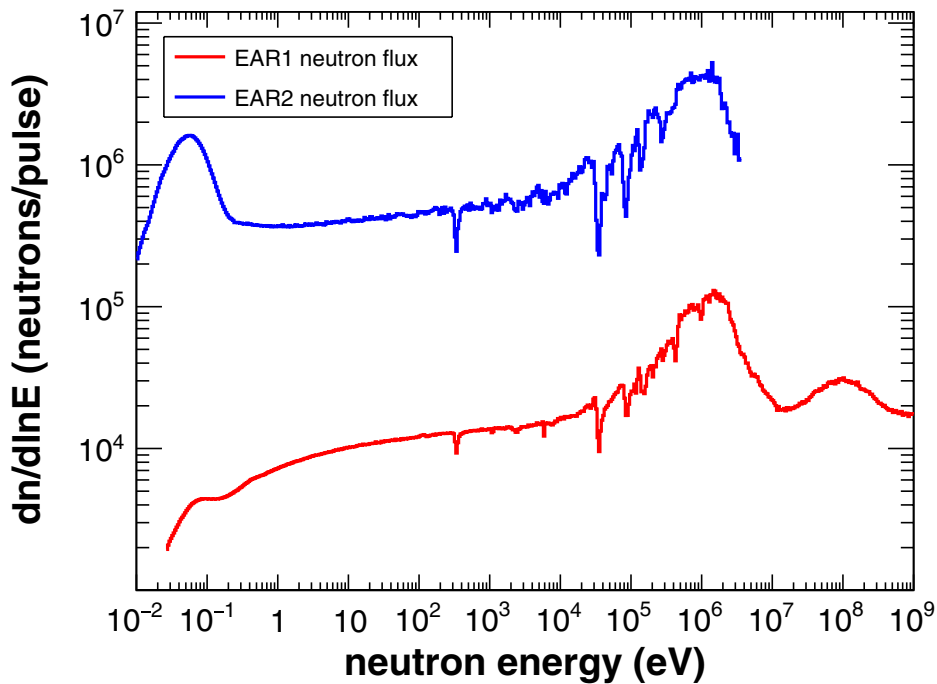


Figure 2. The number of neutrons per equidistant logarithmic energy bin, i.e. per unit of lethargy, ($dn/d\ln E$) per 7×10^{12} protons on target, referred to as “flux”, integrated over the full Gaussian beam profile with a nominal FWHM of 18 mm in EAR1 and 21 mm in EAR2, as seen at the sample position at nominal distances of 185 m (EAR1) and 20 m (EAR2) for the small collimator. The shown fluxes are the preliminary results of several measurements and simulations. The strong reduction of the thermal peak in EAR1 is due to the ^{10}B -loaded moderator.

measurements up to 1 GeV. Furthermore, the position of each fission fragment is also measured, allowing the study of the fission anisotropy. Measurements of the fission cross sections of $^{\text{nat}}\text{Pb}$, ^{209}Bi , ^{232}Th , ^{237}Np , ^{233}U , ^{234}U , relative to ^{235}U and ^{238}U were performed.

During phase-II from 2009 to 2012, the experimental area EAR1 has been upgraded to become a class A work zone, allowing to use unsealed radioactive samples. Both stable and unstable samples were used to measure (n,γ) reactions on ^{25}Mg , ^{54}Fe , ^{56}Fe , ^{57}Fe , ^{58}Ni , ^{62}Ni , ^{63}Ni , ^{92}Zr , ^{93}Zr (for references see Ref. [5]) and ^{236}U [11], ^{238}U [12] and ^{241}Am [13]. The TAC was also used in combination with a MicroMegas detector in a first attempt to measure the $^{235}\text{U}(n,\gamma)$ reaction using a veto on the $^{235}\text{U}(n,f)$ reaction [14]. An upgraded PPAC assembly was used to measure the angular distributions of ^{232}Th and ^{234}U fission fragments. The angular distribution of ^{235}U and ^{238}U [15] and the analysis of the resonance region of the ^{234}U [16] measurement has been reported recently.

Several other techniques have been tested as well, including resonance spin assignments on ^{87}Sr with the TAC, a measurement of the $^{59}\text{Ni}(n,\alpha)$ cross section with diamond detectors [17], and measurements with MicroMegas detectors on $^{240}\text{Pu}(n,f)$, $^{242}\text{Pu}(n,f)$ and $^{33}\text{S}(n,\alpha)$, and a flux-integrated cross section of $^{12}\text{C}(n,p)^{12}\text{B}$.

While tables of the phase-I and phase-II measurements with their references are given in Ref. [5], Table 1 summarizes the measurements performed in both EAR1 and EAR2 in 2014, 2015 and 2016. Additional references for the fission programme can also be found in Ref. [18].

The experimental area EAR2 was designed as a class A work zone, allowing unsealed radioactive samples to be used, for which the n.TOF facility has particularly suited beam properties. For the operation of Phase-III, a new data

Table 1. The nuclear data measurements performed at n.TOF during phase-III in 2014, 2015 and 2016 for both EAR1 and EAR2.

| nucleus | reaction | detector | EAR | ref. |
|-------------------|------------------|------------------------|------------|----------|
| ^7Be | (n,α) | silicon | EAR2 | [19–21] |
| ^7Be | (n,p) | silicon | EAR2 | [21] |
| ^{26}Al | $(n,\alpha/p)$ | silicon | EAR2 | [22] |
| ^{33}S | (n,α) | MGAS | EAR2 | [23] |
| ^{70}Ge | (n,γ) | C_6D_6 | EAR1 | [24] |
| ^{72}Ge | (n,γ) | C_6D_6 | EAR1 | [24] |
| ^{73}Ge | (n,γ) | C_6D_6 | EAR1 | [24] |
| ^{74}Ge | (n,γ) | C_6D_6 | EAR1 | [24] |
| ^{76}Ge | (n,γ) | C_6D_6 | EAR1 | [24] |
| ^{147}Pm | (n,γ) | C_6D_6 | EAR2 | [25] |
| ^{171}Tm | (n,γ) | C_6D_6 | EAR1, EAR2 | [25] |
| ^{204}Tl | (n,γ) | C_6D_6 | EAR1 | [26] |
| ^{233}U | $(n,\gamma/f)$ | TAC | EAR1 | [27] |
| ^{235}U | (n,f) | PRT | EAR1 | [28] |
| ^{235}U | $(n,f)\text{FF}$ | STEFF | EAR2 | [29] |
| ^{237}Np | (n,f) | PPAC | EAR1 | [30] |
| ^{237}Np | (n,f) | MGAS | EAR2 | [30] |
| ^{240}Pu | (n,f) | MGAS | EAR2 | [31, 32] |
| ^{242}Pu | (n,γ) | C_6D_6 | EAR1 | [33, 34] |

acquisition system was developed, based on 175 MSample digitizers with a sampling frequency of up to 2 GHz and amplitude resolution of 12 and 14 bits. The larger on-board memory has significantly increased the exploitable time-of-flight range which is now expanded down to thermal neutron energies for both EAR1 and EAR2.

The measurement programme in EAR2 started with a first part of commissioning by measuring quantities such as flux and background and focussing on the feasibility

of fission measurements. The energy dependence of the number of neutrons incident on the sample, referred to as the neutron flux, was measured both with an in-beam neutron-to-charged-particle converter foil, monitored by off-beam silicon detectors, and foils combined with in-beam MicroMegas detectors.

After the first part of commissioning, the very first physics measurement in EAR2 concerned the $^{240}\text{Pu}(n,f)$ reaction with MicroMegas detectors [31], later followed by a similar setup to measure $^{237}\text{Np}(n,f)$. In 2015, the commissioning of EAR2 continued, exploring the possibilities of (n,γ) measurements, for applications in nuclear astrophysics [35] and nuclear technology, as well as neutron-induced charged particle reactions like the $^7\text{Be}(n,\alpha)$ and $^7\text{Be}(n,p)$ experiments. The complex multi-detector system STEFF [36] was installed in EAR2 for commissioning and a measurement of fission fragments spectroscopy on ^{235}U . Silicon strip detectors were used in EAR2 for a $^{26}\text{Al}(n,\alpha)$ measurement. In EAR1 the use of a proton recoil detector (PRT) was developed in order to measure the $^{235}\text{U}(n,f)/^1\text{H}(n,n)$ ratio. The $^{233}\text{U}(n,\gamma/f)$ ratio was measured with the TAC combined with a fission ionization chamber [27].

4. n_TOF measurements and nuclear evaluations

The majority of the measurements at the n_TOF facility are related to cross sections: capture and fission experiments since phase-I and also (n,α) and (n,p) measurements in phase-II and phase-III. Once an experiment has been fully analyzed and the results published, it is important to make the data available for further use in nuclear data evaluations. The basic measured data for a typical measurement are a set of detector count spectra as a function of neutron time-of-flight. Usually these spectra are then processed in order to obtain a reaction yield or cross section ratio as a function of neutron energy. This is the quantity that is intended to be stored in the EXFOR database, which then subsequently can serve as a basis for nuclear data evaluations, which can be adopted in new releases of evaluated nuclear data libraries. Applications for nuclear technology do not rely directly on measurements as collected in EXFOR, but nearly always on evaluated libraries. The time path between a measurement and the inclusion in an evaluation for an evaluated nuclear data library is in general rather capricious. A list of requests for measurements is organized by the OECD-NEA High Priority Request List (HPRL) [37]. Evaluation efforts are performed in national projects or on an international scale like the CIELO project [38, 39] for the nuclei ^1H , ^{16}O , ^{56}Fe , $^{235,238}\text{U}$, and ^{239}Pu .

In the field of nuclear data much effort is nowadays put on reducing uncertainties. One strategy is to perform the same measurement at different facilities worldwide. Recognizing and documenting measured data, uncertainties and covariances is an additional exertion in this respect. The process of reducing the several independent uncorrelated counting spectra to a single reaction yield or ratio as function of time-of-flight (or neutron energy), introduces off-diagonal covariance elements. While the full covariance matrix of a yield consisting of several thousands of data points becomes too large to report directly in EXFOR, it is sometimes

more convenient to use a vectorized covariance matrix reflecting the full data reduction process [40]. For smaller datasets on the contrary it is very instructive to access the full covariance matrix of a measured spectrum as for example nicely illustrated in Refs. [41, 42]. Nevertheless, when the correlations introduced by the data reduction are small compared to certain common uncertainties, for example related to sample mass or normalization, it may be sufficient to report only these uncertainties separately as "systematic" uncertainties. In any case, in order to make the data in EXFOR useful for evaluations, the description of the experimental details should be as complete as possible [43]. Data submission of n_TOF measurements to EXFOR, which is crucial for its consideration in evaluations, is an ongoing process [44]. A comprehensive list of n_TOF data dissemination is maintained on a webpage [45].

5. Conclusion

The key features for accurate neutron measurements at the n_TOF facility with its two beam lines and experimental areas EAR1 and EAR2 are the large energy range, high neutron-energy resolution, and the high instantaneous neutron flux. EAR2 with its about 25 times higher flux than in EAR1, combined with an additional reduction by a factor 10 of the background due to the sample's radioactivity, significantly enhances the possible measurements on unstable targets at n_TOF. The preparation and characterization of such targets suitable for neutron cross-section measurements is an increasingly complicated task, feasible only in highly specialized laboratories.

The measurements at CERN's neutron time-of-flight facility n_TOF with its unique features contribute substantially to our knowledge of neutron-induced reactions. This goes together with cutting-edge developments in detector technology and analysis techniques, design of challenging experiments, and training of a new generation of physicists working in neutron physics. This work has been actively supported since the beginning of n_TOF by the European Framework Programmes [46]. One of the future developments currently being studied is a possible upgrade of the spallation target in order to optimize the characteristics of the neutron beam in EAR2. The n_TOF collaboration, consisting of about 150 researchers from 40 institutes, continues its scientific programme in both EAR1 and EAR2, in this way continuing its 15 years history of measuring high-quality neutron-induced reaction data.

References

- [1] N. Otuka et al., Nucl. Data Sheets **120**, 272 (2014)
- [2] V. Semkova et al., these proceedings **R494** (2016)
- [3] C. Weiß et al., Nucl. Instr. Meth. A **799**, 90 (2015)
- [4] E. Chiaveri et al., these proceedings **I217** (2016)
- [5] F. Gunsing (The n_TOF Collaboration) et al., Eur. Phys. J. Plus **131**(10), 371 (2016), <http://dx.doi.org/10.1140/epjpp/i2016-16371-4>
- [6] C. Rubbia et al., CERN/LHC/98-02 (1998)
- [7] C. Borcea et al., Nucl. Instrum. Methods Phys. Res. Sect. A **513**, 524 (2003)
- [8] D. Schumann et al., these proceedings **I297** (2016)
- [9] G. Sibbens et al., these proceedings **R299** (2016)

- [10] J. Pancin et al., Nucl. Instr. Meth. A **524**(1-3), 102 (2004)
- [11] M. Mastromarco et al., these proceedings **S031** (2016)
- [12] F. Mingrone et al., these proceedings **R118** (2016)
- [13] E. Mendoza et al., these proceedings **R036** (2016)
- [14] J. Balibrea et al., these proceedings **R028** (2016)
- [15] E. Leal-Cidoncha et al., EPJ Web of Conferences **111**, 10002 (2016)
- [16] E. Leal-Cidoncha et al., these proceedings **S416** (2016)
- [17] C. Weiss et al., Nucl. Data Sheets **120**(0), 208 (2014)
- [18] A. Tsinganis et al., Physics Procedia **64**, 130 (2015)
- [19] L. Cosentino et al., Nucl. Instr. Meth. A **830**, 197 (2016)
- [20] M. Barbagallo et al., Phys. Rev. Lett. **117**, 152701 (2016)
- [21] N. Colonna et al., these proceedings **R046** (2016)
- [22] C. Lederer et al., Proposal CERN-INTC-2014-006/INTC-P-406 (2014)
- [23] M. Sabaté-Gilarte et al., these proceedings **R047** (2016)
- [24] C. Lederer et al., Proposal CERN-INTC-2013-021/INTC-P-381 (2013)
- [25] C. Guerrero et al., these proceedings **R042** (2016)
- [26] C. Guerrero et al., Proposal CERN-INTC-2014-003/INTC-P-404 (2014)
- [27] M. Bacak et al., these proceedings **S131** (2016)
- [28] L. Cosentino et al., these proceedings **S132** (2016)
- [29] J.A. Ryan et al., these proceedings **R171** (2016)
- [30] L. Audouin et al., Proposal CERN-INTC-2015-007/INTC-P-431 (2015)
- [31] A. Tsinganis et al., in *14th Int. Conf. Nucl. Reac.*, edited by F. Cerutti et al. (CERN-Proc.-2015-001, 2015), pp. 21–26
- [32] A. Stamatopoulos et al., these proceedings **R093** (2016)
- [33] J. Lerendegui-Marco et al., EPJ Web of Conferences **111**, 02005 (2016)
- [34] J. Lerendegui-Marco et al., these proceedings **S032** (2016)
- [35] G. Tagliente et al., in *14th Int. Conf. Nucl. Reac.*, edited by F. Cerutti et al. (CERN-Proc.-2015-001, 2015), pp. 267–274
- [36] A.J. Pollitt et al., EPJ Web of Conferences **93**, 02018 (2015)
- [37] <https://www.oecd-nea.org/dbdata/hpr1>
- [38] M.B. Chadwick et al., Nucl. Data Sheets **118**, 1 (2014)
- [39] M. Chadwick et al., these proceedings **PL499** (2016)
- [40] B. Becker et al., J. of Instr. **7**, P11002 (2012)
- [41] C. Sage et al., Phys. Rev. C **81**(6), 064604 (2010)
- [42] X. Ledoux et al., Ann. of Nucl. En. **76**, 514 (2015)
- [43] F. Gunsing et al., Tech. Rep. IAEA INDC(NDS)-0647 (2013)
- [44] E. Dupont et al., these proceedings **R493** (2016)
- [45] <http://twiki.cern.ch/NTOFPublic>
- [46] E. Gonzalez et al., these proceedings **I059** (2016)